Materials Chemistry and Physics 126 (2011) 711–716

Contents lists available at ScienceDirect

Materials Chemistry and Physics

journal homepage: www.elsevier.com/locate/matchemphys

Electrochromic performance of mixed V_2O_5–MoO_3 thin films synthesized by pulsed spray pyrolysis technique

C.E. Patil[a], P.R. Jadhav[b], N.L. Tarwal[b], H.P. Deshmukh[c], M.M. Karanjkar[d], P.S. Patil[b,*]

[a] Department of Physics, Bharati Vidyapeeth's MBSK Kanya Mahavidyalay, Kadegaon, Sangli, MS, India
[b] Thin Film Materials Laboratory, Department of Physics, Shivaji University, Kolhapur 416004, India
[c] Bharati Vidyapeeth's Y M College, Pune, MS, India
[d] Vivekanand College, Kolhapur, India

ARTICLE INFO

Article history:
Received 11 August 2010
Received in revised form
19 November 2010
Accepted 13 December 2010

Keywords:
Oxides
Semiconductors
Thin films
Optical properties

ABSTRACT

Mixed V_2O_5–MoO_3 thin films were deposited onto the glass and fluorine doped tin oxide (FTO) coated glass substrates, at 400 °C by pulsed spray pyrolysis technique (PSPT). Equimolar vanadium chloride (VCl_3) and ammonium molybdate aqueous solutions were mixed together in volume proportions (5–15% molybdenum) and used as a precursor solution for the deposition of mixed V_2O_5–MoO_3 thin films. The structural, morphological, optical and electrochromic properties of the films deposited at different Mo concentrations were studied. With increase in the percentage of Mo the peaks belonging to tetragonal phase of V_2O_5 eventually disappear and the (1 0 1) orthorhombic V_2O_5 phase is observed. Scanning electron microscopy (SEM) shows micro thread like reticulated morphology. The optical band gap energy varied over 2.91–2.85 eV. All the films exhibited cathodic electrochromism in lithium containing electrolyte (0.5 M $LiClO_4$ + propylene carbonate (PC)). The highest coloration efficiency (CE) for the V_2O_5 film with 15% MoO_3 mixing was found 35.27 $cm^2\ C^{-1}$.

1. Introduction

Electrochromism (EC) is a phenomenon in which materials are able to change their optical properties in a reversible and persistent way under the action of a voltage pulse [1]. Potential advantages offered by electrochromic materials include a long open circuit memory and low power requirement. EC has attracted a growing amount of interest because it can be used in electrochromic devices for several applications: energy efficient glazing, privacy glass, partitions, skylights, large area displays and automotive glazing including sunroofs and mirrors. Transition metal oxides such as tungsten trioxide (WO_3) [2], molybdenum oxide (MoO_3) [3], iridium oxide (lrO_2) [4] and vanadium pentaoxide (V_2O_5) [5] have been widely used as inorganic electrochromic materials and are based on a reversible change in the optical properties during electrochemical oxidation or reduction processes. The electrochromic behavior can be explained by a combinational injection and extraction of electrons and ions. During an electrochromic process, at a given voltage, electrons are injected (reduction) or extracted (oxidation) and at the same time, ions are moved into or out of the electrochromic materials to balance charge neutrality.

Among those transition metal oxides, WO_3 appears to be best electrochromic compound [6]. However, for building applications the bright blue color of WO_3 films in the reduced state is not as favorable as bronze or pile yellow colors for most building applications. V_2O_5 shows pile yellow in colored state, hence technologically interested.

Day and Sullivan reported V_2O_5 was as a cathode material [7]. It is an interesting cathode material because (i) it offers high specific energy density [8], (ii) it undergoes reversible topotactic reaction with lithium [9] and (iii) it has a higher electrochemical activity with the highest stability [10]. Also, V_2O_5 exhibits dual (anodic and cathodic) electrochromism [1], but it has poor CE. One approach for improving the CE of V_2O_5 films is through doping/mixing with other oxides with high electrochromic performance. As many papers reported, electrochromic metal oxide thin films 'doped' with other oxides are superior to pure-oxide electrochromes in being more robust than the constituents oxides alone [11].

MoO_3 is one of the most studied electrochromic materials. It offers higher CE, but have relatively lower electrochemical stability. The interaction between V_2O_5 and MoO_3 is unique because of the similarities of ionic radii and the structure in their highest oxidation state.

However, these applications depend on the techniques used to grow the films and the performance linked with the crystallinity and morphology of the films [12]. The V_2O_5 thin films were prepared by different techniques such as rf-sputtering [13],

* Corresponding author. Tel.: +91 231 2609230; fax: +91 231 26091533.
E-mail address: psp_phy@unishivaji.ac.in (P.S. Patil).

0254-0584/$ – see front matter © 2010 Elsevier B.V. All rights reserved.
doi:10.1016/j.matchemphys.2010.12.055

dc-magnetron sputtering [14], flash evaporation [15], etc. Sol–gel technique [16] and pulsed laser deposition [17]. However, the PSPT with relatively low cost and large area have been used for the first time to prepare this material.

In this study, we report the deposition of mixed V_2O_5–MoO_3 thin films and their electrochromic properties. The purpose of this work was to enhance the coloration efficiency, charge capacity and reduce the cost of V_2O_5 by doping appropriate ratio of MoO_3.

2. Experimental

The MoO_3 mixed V_2O_5 thin films were grown on FTO coated glass and soda-lime glass substrates by using PSPT, patented by us [18]. It is a novel spray pyrolysis technique that facilitates judicious control over preparative parameters. Films deposited on glass substrates were used for structural and morphological characterization whereas those deposited onto the FTO-coated glass substrates were used for electrochromic characterization. The preparative parameters of V_2O_5 thin films deposited using the PSPT has been reported by us [19]. In brief, the precursor solution was sprayed on to the pre-heated glass substrates maintained at a desired substrate temperature (400 °C) with compressed air, at the flow rate of 18 l min^{-1}, was used as a carrier gas. The nozzle to substrate distance was optimized at 22 cm. 20 ml of the precursor solution used for the deposition of the films was prepared by adding following solutions in an appropriate ratio:

(1) Solution A: VCl_3 powder dissolved in methanol and 0.005 M solution was prepared.
(2) Solution B: pure MoO_3 powder dissolved in ammonia and diluted with distilled water at room temperature.

An adequate quantity of the solutions A and B were added and the final solution (20 ml) was pneumatically pulverized on the glass and FTO coated conducting glass substrates heated at 400 °C. The 5%, 10% and 15% MoO_3-mixed V_2O_5 samples were referred as (VM_1), (VM_2) and (VM_3) respectively. V_2O_5 without MoO_3 mixture is denoted as (V_0).

The thickness of the MoO_3 mixed V_2O_5 thin films V_0, VM_1, VM_2 and VM_3 deposited at 400 °C was determined using fully computerized AMBIOS Make XP-1 surface profiler with 1 Å vertical resolution and is found to be ~132 nm, 320 nm, 339 nm and 368 nm, respectively.

The powder collected from the deposited film was characterized by infrared (IR) spectroscopy using the Perkin Elmer IR spectrometer model 783 in the spectral range 450–4000 cm^{-1}. To record IR patterns, the pellet was prepared by mixing KBr with V_2O_5 powder, collected from a thin film, in the ratio 300:1 and then pressing the pellet between two pieces of polished steel. The structural and morphological characterizations were carried out using X-ray diffractometer (Philips Model PW 3710) with Cu Kα radiation (wavelength 1.5432 Å) and scanning electron microscopy (JEOL Model JSM-6360), respectively. The optical absorption and transmittance spectra were recorded using UV–vis spectrophotometer (Systronics Model 119) in the wavelength range of 350–850 nm.

The electrochemical cell consists of a conventional three-electrode configuration cell, in which the V_2O_5 thin film deposited on to FTO coated glass substrate (15–20 Ω cm^{-1}), a graphite plate and a saturated calomel electrode (SCE) served respectively as working electrode, counter electrode and the reference electrode. A 0.5 M $LiClO_4$ + PC was used as an electrolyte solution. The cyclic voltammetry (CV), chronoamperometry (CA) and chronocoulometry (CC) experiments were carried out using a VersaStat-II (EG&G) potentiostat/galvanostat, controlled by M270 software. All the potentials were referred with respect to SCE.

3. Results and discussion

3.1. FT-IR study

The IR transmittance spectrum presents information about phase composition as well as the way oxygen is bound to the metal ions (M–O structure). The FT-IR transmittance spectrum of the powder collected from the film in the range 450–4000 cm^{-1} is shown in Fig. 1. The spectrum comprises 11 stretching vibrations at different wave numbers such as: (i) 588 cm^{-1}, (ii) 769 cm^{-1}, (iii) 940 cm^{-1}, (iv) 1178 cm^{-1}, (v) 1394 cm^{-1}, (vi) 1461 cm^{-1}, (vii) 1633 cm^{-1}, (viii) 1735 cm^{-1}, (ix) 2861 cm^{-1}, (x) 2928 cm^{-1} and (xi) 3565 cm^{-1}. The existence of (iii) and (iv) bands corresponds to the stretching vibration of unshared V=O bonds while bands appear at (i) and (ii) are attributed to the stretching vibration of Mo=O bond. The bands (vi), (vii) and (xi) indicate that a small amount of the water content.

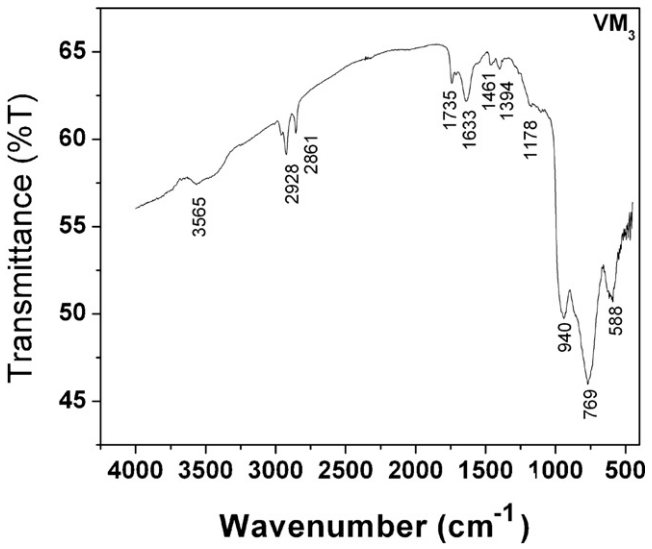

Fig. 1. The IR spectrum of the MoO_3–V_2O_5 thin film (VM_3) deposited at 400 °C.

3.2. X-ray diffraction

The structural identification and changes in crystallinity of V_2O_5 thin films with the concentration of MoO_3 were studied with XRD technique. The XRD was carried out in the range of diffraction angle 2θ between 20° and 80°. The XRD patterns of V_2O_5 thin films doped with 5%, 10% and 15% MoO_3 at 400 °C temperature as shown in Fig. 2. It was found that with increase in percentage of Mo the peaks belonging to tetragonal phase of V_2O_5 eventually disappear and the (1 0 1) orthorhombic V_2O_5 phase is observed. From the spectra, it is observed that the sample VM_3 shows amorphous nature with a broad hump centered at 27 °C. For all the samples, no reflections belonging to MoO_3 were observed. As mixing percentage of MoO_3 increases the (1 0 1) peak intensity decreases and finally this peak vanishes for VM_3. For VM_3 sample, we observed the amorphous phase formation with no characteristic peak for V_2O_5 and MoO_3. The addition of MoO_3 thus can rupture the crystalline character of V_2O_5 and lead to amorphous nature, favorable for electrochromic ion intercalation/deintercalation processes. The calculated values of crystallite size by using the well known Debey–Scherrer's formula are 11, 10 and 9 nm for sample VM_1, VM_2 and VM_3, respectively.

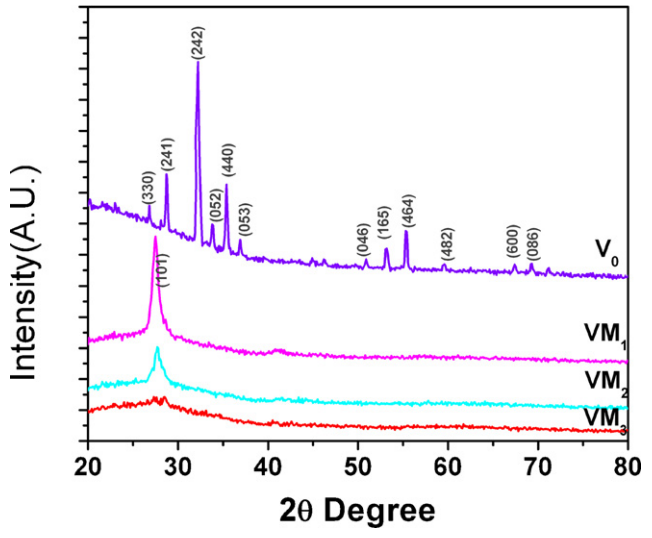

Fig. 2. XRD spectra recorded for samples V_0, VM_1, VM_2 and VM_3 deposited at 400 °C.

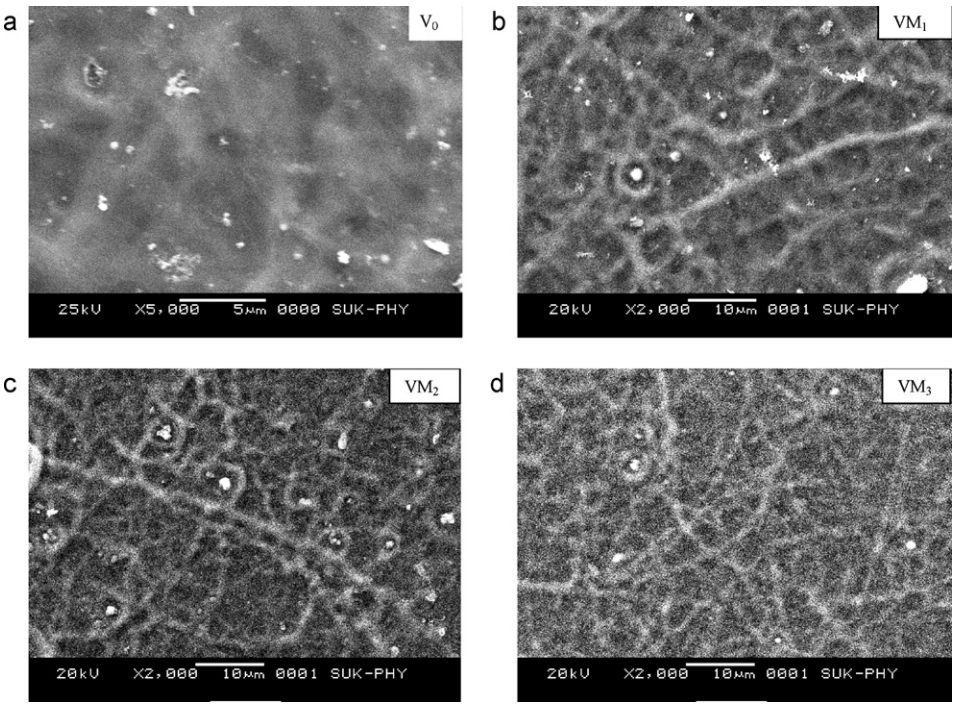

Fig. 3. SEM micrograph for samples (a) V_0, (b) VM_1, (c) VM_2 and (d) VM_3 deposited at 400 °C.

3.3. SEM

V_2O_5 thin films were analyzed by SEM to determine the influence of the MoO_3 concentration on the morphology. Fig. 3(a)–(d) shows SEM images of V_0, VM_1, VM_2 and VM_3 samples. Changes in the film morphology with the doping percentage were observed. Micro thread like reticulated morphology was observed with average thread width from ~2 μm to 0.9 μm. Sample VM_1 exhibits onset of characteristic growth of MoO_3 in fibrous reticulated network. Sample VM_1 also shows few spherical grains of size varying from 2 to 3 μm on the surface. Sample VM_2 shows decrease in the width of fiber. The fibers of width 1–2 μm and length several micrometers were observed for sample VM_3.

3.4. Optical studies

The optical absorption spectra for all samples were recorded in wavelength range of 350–850 nm at room temperature. In order to confirm the nature of optical transition in these samples, the optical data were analyzed using classical Eq. (1) [20]:

$$\alpha = \frac{\alpha_0(h\upsilon - E_g)^n}{h\upsilon} \quad (1)$$

where E_g is the optical band gap energy, $h\nu$ is the photon energy and n is the constant. For allowed direct transitions $n = 1/2$. The plots of $(\alpha h\nu)^2$ against $h\nu$ for all samples are shown in Fig. 4. The nature of the plot suggests direct interband transition. The extrapolation of straight-line portions to zero absorption coefficient ($\alpha = 0$) leads to the estimation of band gap energy values. These values are listed in Table 1. It is noted that, the band gap energy increases from 2.85 eV (VM_1 samples) to 2.91 eV with increase in MoO_3 content. The observed increase in the band gap can be attributed to quantum confinement, in the disordered structure.

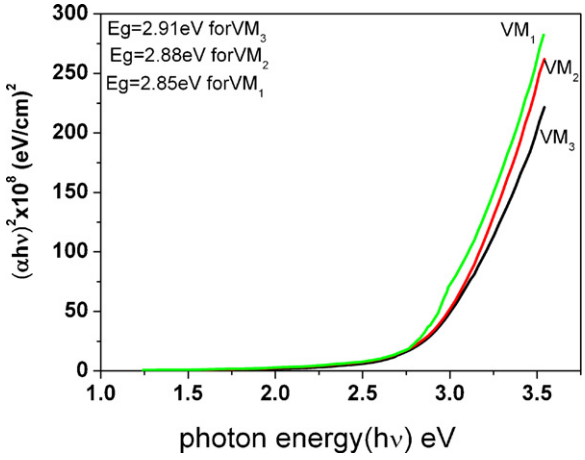

Fig. 4. Plot of $(\alpha h\nu)^2$ versus $(h\nu)$ of VM_1, VM_2 and VM_3 samples.

3.5. Electrochemical measurements

3.5.1. Cyclic voltammetry (CV)

The potential was cycled from +1.5 to −0.5 V (versus SCE) at potential sweep rate 100 mV s^{-1} in 0.5 M ($LiClO_4$ + PC). During the

Table 1
Various electrochromic parameters calculated from electrochemical and iono-optical studies of MoO_3-mixed V_2O_5 thin films.

Sample code	T_b	T_c	Q_i (mC cm^{-2})	Q_{di} (mC cm^{-2})	ΔOD	Reversi bility (%)	Coloration efficiency (cm^2 C^{-1})	Diffusion constant, D (cm^2 s^{-1})
V_0	20	23	24	22	0.14	95.59	14.96	1.129×10^{-18}
VM_1	46.39	32.14	19.98	13.69	0.16	68.50	19.96	2.17×10^{-18}
VM_2	52.36	30.06	20.21	12.64	0.24	62.54	29.81	2.098×10^{-18}
VM_3	48.39	23.50	22.24	13.75	0.31	61.83	35.27	1.897×10^{-17}

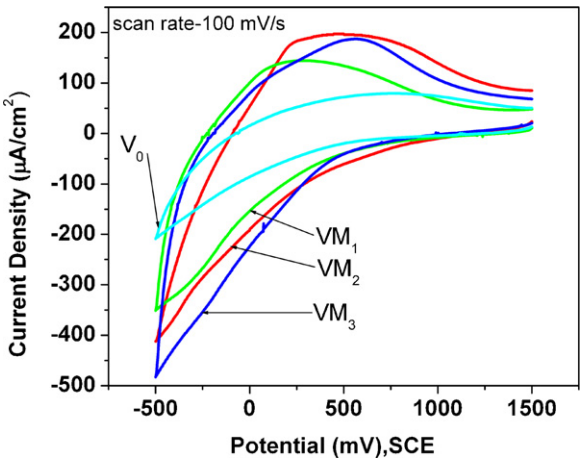

Fig. 5. CV recorded for V_0, VM_1, VM_2 and VM_3 samples.

potential sweep the current resulting from ion intercalated and deintercalated was recorded and the variation is shown in Fig. 5. At the cathodic potential end (−0.5 V), the film is in the bleached state and at the anodic potential end (+1.5 V), it acquires colored state. The bleaching and coloration of MoO_3–V_2O_5 thin films is associated with intercalation and deintercalation of Li^+ ions and electrons in the film. It is observed that, with increase in MoO_3 concentration the cathodic peak current density shifts from −347 to −484 μA cm^{-2}. The increase in the area of voltammograms with increase in MoO_3 content suggests that the structure offers an easy way to diffusion and charge transfer process of ions. For all the samples, diffusion constant is calculated using relation (2).

The diffusion of Li^+ ions is calculated from Randles–Servcik equation:

$$i_p = 2.72 \times 10^5 \times n^{3/2} \times D^{1/2} \times C_0 \times \nu^{1/2} \quad (2)$$

where D is the diffusion coefficient, C_0 is the concentration of active ions in the solution, ν is the scan rate, n is the number of electrons assumed to be 1 and i_p is the peak current density.

With respect to increase in MoO_3 content, the diffusion coefficient increases of the order of 10^{-18} cm^2 s^{-1} as compared to pure V_2O_5 film. The diffusion coefficient depends on the conductivity (σ) of diffusing ionic species (Li^+), the nature of film (crystallinity, porosity, hydration) and the electrolyte. The values of diffusion coefficient calculated for all the samples are mentioned in Table 1. Fig. 6 shows variation of i_p with respect to MoO_3 content. With increase in MoO_3 content both i_p increases. Linear variation of i_p with root scan rate indicates that the cyclic process is diffusion controlled.

3.5.2. Chronoamperometry (CA)

Potential step experiments were carried out to determine the kinetics of reduced-oxidation reaction. The speed with which EC devices can be switched from one state to another state is great importance for determining its application capability. Here, CA cycling was performed on MoO_3–V_2O_5 film between +0.5 V and −0.5 V versus SCE for 60 s and the resultant current–time response for the sample V_0, VM_1, VM_2 and VM_3 is shown in Fig. 7.

From the current versus time transients, it is clearly observed that both coloration current (i_c) and bleaching current (i_b) following the step was smooth and decreased continuously with time.

This decrease in current with time has been used to measure the speed of EC response of MoO_3–V_2O_5 oxide thin films. The coloration time (t_c) and bleaching time (t_b) were calculated from the current time transients. From figure, it is observed that as MoO_3 content increases the coloration-bleaching kinetics becomes easier and faster. The response time for all the samples is calculated from the CA plots and is reported in Table 2.

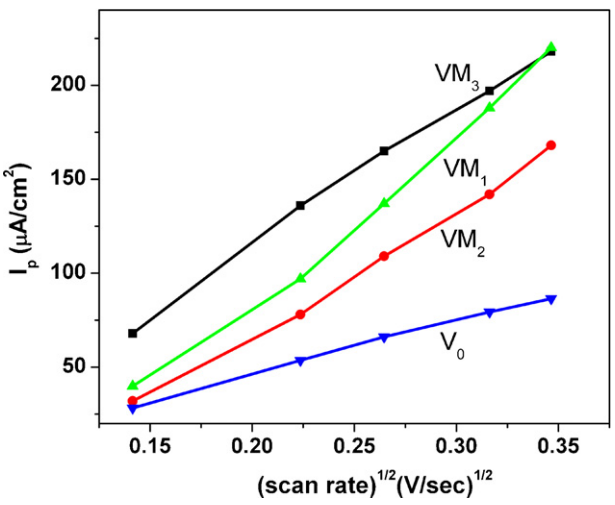

Fig. 6. Plots of anodic and cathodic peak currents versus square root of scan rates for V_0, VM_1, VM_2 and VM_3 samples.

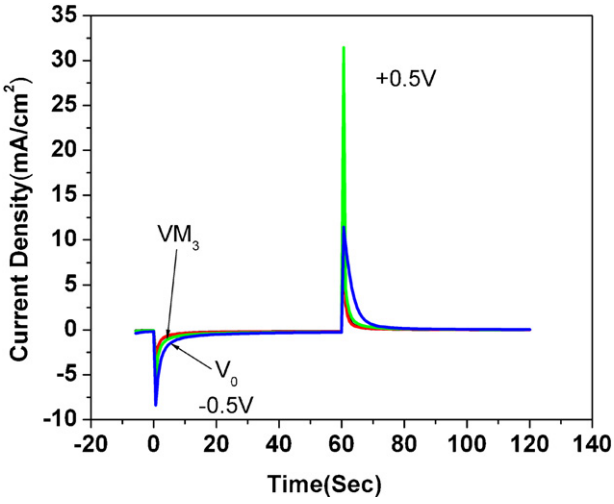

Fig. 7. CA curves obtained for V_0, VM_1, VM_2 and VM_3 samples.

3.5.3. Chronocoulometry (CC)

To study Li^+ ion intercalation–deintercalation process with respect to time, chronocoulometry was carried out. Charges intercalated–deintercalated versus time transients for all films at ±0.5 V (SCE) for a step of 60 s is shown in Fig. 8. In the forward scan the charges are intercalated into the film by diffusion process, resulting in coloration due to reduction of V^{5+} to V^{4+} and Mo^{6+} to Mo^{5+} states. In the reverse scan, the intercalated charge is removed from the film, resulting in bleaching due to oxidation of V^{4+} to V^{5+} and Mo^{5+} to Mo^{6+} states.

Table 2
Thickness, band gap and response time from CA are determined for MoO_3-mixed V_2O_5 thin films.

Sample ID	Thickness, t (nm)	Band gap, E_g (eV)	Response time	
			t_c (s)	t_b (s)
VM_1	320	2.91	10.76	9
VM_2	339	2.88	9	11
VM_3	368	2.85	9	11

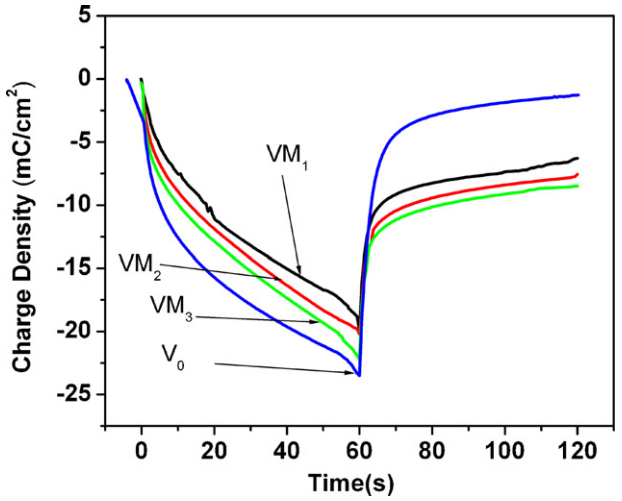

Fig. 8. CC curves obtained for V_0, VM_1, VM_2 and VM_3 samples.

From CC curves, the amount of charge intercalated (Q_i), amount of charge deintercalated (Q_{di}) and hence residual charge ($Q_i - Q_{di}$) has been calculated. The electrochromic reversibility of the films calculated as the ratio of charge deintercalated (Q_{di}) to charge intercalated (Q_i). It is remarkably observed that, the reversibility decreases with MoO_3 content increases.

3.5.4. Iono-optical studies

Fig. 9 shows the transmittance spectra for all the samples in their colored and bleached states were recorded in the wavelength range of 350–1000 nm, at the room temperature. The optical absorption by thin layer is described by the dimensionless quantity (α_t), which is called as optical density (OD). The change in optical density (ΔOD) and CE are calculated using relation (3) and (4) respectively:

$$\Delta OD = \ln\left(\frac{T_b}{T_c}\right) \tag{3}$$

where T_b and T_c are the transmittance of the V_2O_5 films in its colored and bleached states, respectively. The CE is defined as the change in optical density per unit-inserted charge and it is calculated using relation (4):

$$CE = \frac{\Delta OD}{Q_i} = \frac{\ln[T_b/T_c]_{\lambda=630\,nm}}{q/A} \tag{4}$$

where Q_i is the amount of charge intercalated in the sample to cause change in optical density, which was estimated by integrating the area under the curve of current density versus time.

It has been observed that with increase in MoO_3 content transmittance modulation (ΔT) increases, which improves OD and hence CE increases from 14.96 to 35.27 $cm^2\,C^{-1}$. Various electrochromic parameters derived from electrochemical characterization of spray deposited MoO_3-mixed V_2O_5 thin films are given in Table 1.

Hence, it is concluded that VM_3 sample exhibits better electrochromic properties by virtue of having greater MoO_3 content. Further experiment on increasing MoO_3 content in V_2O_5 failed due to the formation of powdery (inferior) quality films. Therefore, 15% mixing of MoO_3 is an optimum amount to yield better electrochromic properties of V_2O_5 thin films, deposited by using PSPT.

4. Conclusions

MoO_3 mixing effects in electrochromic V_2O_5 thin films synthesized using PSPT have been investigated. With increasing MoO_3 content, the structure of V_2O_5 undergoes a phase transformation from tetragonal to orthorhombic with nano-sized grains. It is observed that MoO_3 mixing concentration induced local strain effects are dominated in stabilizing structure. It is seen that MoO_3-mixing can lead to significant surface morphology changes in V_2O_5 films. The fibrous threads like morphology with decreasing width are observed with increasing MoO_3 content. It was found that the CE increases and for sample VM_3 exhibits best electrochromic properties (CE = 35.27 $cm^2\,C^{-1}$). This enhancement in the CE is attributed to the defects and disorder produced in the films due to MoO_3

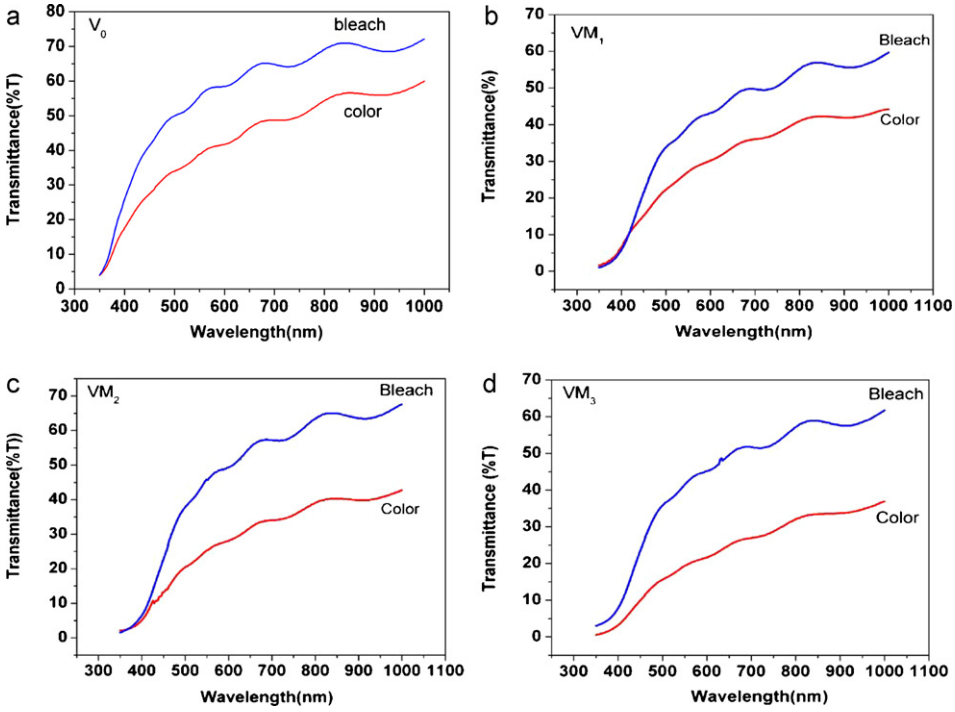

Fig. 9. Transmittance spectra (a) V_0, (b) VM_1, (c) VM_2 and (d) VM_3 samples in its colored and bleached state.

mixing. Hence, we have successfully demonstrated formation of an adequate host for electrochromic devices with MoO_3-mixed V_2O_5 samples.

Acknowledgements

One of the author NLT, wish to acknowledge the University Grants Commission for research fellowship in sciences for meritorious students and CEP is grateful to Bharati Vidyapeeth University, Pune.

References

[1] C.G. Granqvist, Handbook of Inorganic Electrochromic Materials, Elsevier, Amsterdam, 1995.
[2] S.R. Bathe, P.S. Patil, Sol. Energy Mater. Sol. Cells 91 (2007) 1097.
[3] R.S. Patil, M.D. Uplane, P.S. Patil, Appl. Surf. Sci. 252 (2006) 8050.
[4] P.S. Patil, R.K. Kawar, S.B. Sadale, Electrochim. Acta 50 (2005) 2527.
[5] Z. Liu, G. Fang, Y. Wang, Y. Bai, K.L. Yao, J. Phys. D: Appl. Phys. 33 (2000) 2327.
[6] S.S. Kalagi, D.S. Dalavi, R.C. Pawar, N.L. Tarwal, S.S. Mali, P.S. Patil, J. Alloys Compd. 493 (2009) 335.
[7] A.N. Day, B.P. Sullivan, U.S. Patent 3,655,585 (1972).
[8] D.W. Murphy, P.A. Christian, F.J. Disalvo, J.V. Waszezak, Inorg. Chem. 18 (1979) 2800.
[9] S.C. Baker, C.K. Huang, R.A. Huggins, Proc. Electrochem. Soc. 88 (1988) 44.
[10] Y.S. Lin, C.W. Tsai, Surf. Coat. Technol. 202 (2008) 5641.
[11] Y.M. Li, T. Kudo, Sol. Energy Mater. Sol. Cells 39 (1995) 179.
[12] C. Julien, J.P. Guesdon, A. Gorenstein, A. Khelfa, I. Ivanov, Appl. Surf. Sci. 90 (1995) 389.
[13] L. Ottaviano, A. Pennisi, F. Simone, A.M. Salvi, Opt. Mater. 27 (2004) 307.
[14] M.G. Krishna, Y. Debauge, A.K. Bhattacharya, Thin Solid Films 312 (1998) 116.
[15] L. Murawski, C. Sanchez, J. Livage, J.P. Audiers, J. Non-Cryst. Solids 124 (1990) 71.
[16] A. Cremonesi, D. Bersani, P.P. Lottici, Y. Djaoued, R. Brüning, Thin Solid Films 515 (2006) 1500.
[17] S. Beke, S. Giorgio, L. Kőrösi, L. Nánai, W. Marine, Thin Solid Films 516 (2008) 4659.
[18] P.S. Patil, S.B. Sadale, An improved spray pyrolysis process for the preparation of good quality thin film semiconducting coatings and apparatus therefore Indian patent No 214163, 2008.
[19] C.E. Patil, N.L. Tarwal, P.S. Shinde, H.P. Deshmukh, P.S. Patil, J. Phys. D: Appl. Phys. 42 (2009) 025404.
[20] I.M. Tsidilkovsk, Band Structure of Semiconductors, Pergamam Press, Oxford, 1982.